

# One Novel Type of Miniaturization FBG Rotation Angle Sensor With High Measurement Precision and Temperature Self-Compensation

Shanchao JIANG<sup>1\*</sup>, Jing WANG<sup>2</sup>, and Qingmei SUI<sup>2</sup>

<sup>1</sup>*School of Electrical Engineering, Yancheng Institute of Technology, Yancheng, 224051, China*

<sup>2</sup>*School of Control Science and Engineering, Shandong University, Jinan, 250061, China*

\*Corresponding author: Shanchao JIANG      Email: jiangshanchao88624@126.com

**Abstract:** In order to achieve rotation angle measurement, one novel type of miniaturization fiber Bragg grating (FBG) rotation angle sensor with high measurement precision and temperature self-compensation is proposed and studied in this paper. The FBG rotation angle sensor mainly contains two core sensitivity elements (FBG1 and FBG2), triangular cantilever beam, and rotation angle transfer element. In theory, the proposed sensor can achieve temperature self-compensation by complementation of the two core sensitivity elements (FBG1 and FBG2), and it has a boundless angle measurement range with  $2\pi$  rad period due to the function of the rotation angle transfer element. Based on introducing the joint working processes, the theory calculation model of the FBG rotation angle sensor is established, and the calibration experiment on one prototype is also carried out to obtain its measurement performance. After experimental data analyses, the measurement precision of the FBG rotation angle sensor prototype is  $0.2^\circ$  with excellent linearity, and the temperature sensitivities of FBG1 and FBG2 are  $10 \text{ pm}/^\circ\text{C}$  and  $10.1 \text{ pm}/^\circ\text{C}$ , correspondingly. All these experimental results confirm that the FBG rotation angle sensor can achieve large-range angle measurement with high precision and temperature self-compensation.

**Keywords:** Rotation angle; FBG; temperature self-compensation

---

Citation: Shanchao JIANG, Jing WANG, and Qingmei SUI, "One Novel Type of Miniaturization FBG Rotation Angle Sensor With High Measurement Precision and Temperature Self-Compensation," *Photonic Sensors*, 2018, 8(1): 88–96.

---

## 1. Introduction

Rotation angle measurement with high precision has a large demand in many application fields, for example, precision machining, aerospace, and military fields [1]. At present, mature technologies of traditional rotation angle measurement methods mainly include mechanical way and electromagnetic type. Most of these traditional rotation angle measurement methods [2–5], such as polygon apparatus and circle grating, are manual or contact

measurement, and its detection accuracy and stability are easily affected by external environment. With the development of the detection technology, some other rotation angle measurement methods have been developed such as resistance strain type, inductance type, capacitance type, photoelectric coding type, and reluctance type. Meanwhile, some of these measurement methods have certain limitations, such as high requirements for installation, need of the standard components, complex fabrication process, and very expensive

Received: 20 November 2017 / Revised: 9 December 2017

© The Author(s) 2017. This article is published with open access at Springerlink.com

DOI: 10.1007/s13320-017-0483-4

Article type: Regular

cost. All these limitations restrict the application of these measurement methods. Due to its unique advantages, such as immunity to electromagnetic interference, light weight, compact size, resistance to corrosion, and high sensitivity, the fiber Bragg grating (FBG) can solve all these above mentioned limitations and has been used to achieve many engineering parameter measurements, for example, displacement [6], strain [7], and pressure [8]. Despite all this, there are few reports about the research on the FBG rotation angle sensor. To fill the gap, one novel type of miniaturization FBG rotation angle sensor with high measurement precision and temperature self-compensation is proposed in this paper.

The FBG rotation angle sensor mainly contains two core sensitivity elements (FBG1 and FBG2), one triangular cantilever beam, and one rotation angle transfer element. According to the design structure, the proposed sensor can achieve temperature self-compensation due to the complementation of the two core sensitivity elements (FBG1 and FBG2), and it has a boundless angle measurement range with  $2\pi$ rad period due to the function of the rotation angle transfer element, theoretically. Based on introducing the joint working processes, a theory calculation model of the FBG rotation angle sensor is established. To obtain its rotation angle detection performance and temperature compensation performance, the rotation angle and temperature calibration experiments on one sensor prototype are all carried out. After experimental data analyses, the measurement precision of the proposed sensor is  $0.2^\circ$  with excellent linearity, and the rotation angle measurement sensitivities of FBG1 and FBG2 are  $2.5 \text{ pm}/^\circ$  and  $2.6 \text{ pm}/^\circ$ , respectively. The temperature sensitivities of FBG1 and FBG2 are  $10 \text{ pm}/^\circ\text{C}$  and  $10.1 \text{ pm}/^\circ\text{C}$ , correspondingly. All these experimental results confirm that the FBG rotation angle sensor can achieve large-range angle measurement with high precision and temperature self-compensation.

So, the proposed sensor has certain application value in the rotation angle measurement.

## 2. Sensing principle

### 2.1 Composition and structure of the rotation angle sensor

The FBG rotation angle sensor is made up of two fiber Bragg gratings (FBGs), one triangular cantilever beam, one rotating shaft, one angle dial, one rotation angle transfer element, one protective envelope, and some other fixing holes, just as shown in Fig. 1. These two FBGs which are chosen as core sensitivity elements of the FBG rotation angle sensor are marked as FBG1 and FBG2. FBG1 and FBG2 which can be used to achieve temperature self-compensation are separately glued to the upper and lower surfaces of the cantilever beam. The rotation angle transfer element which is the key conversion element of the proposed rotation angle sensor can achieve the transformation between its surface displacement change and the external rotation angle. Further, the rotating shaft can achieve the transformation between the surface strain of triangular cantilever beam and surface displacement of the rotation angle transfer element. The angle dial

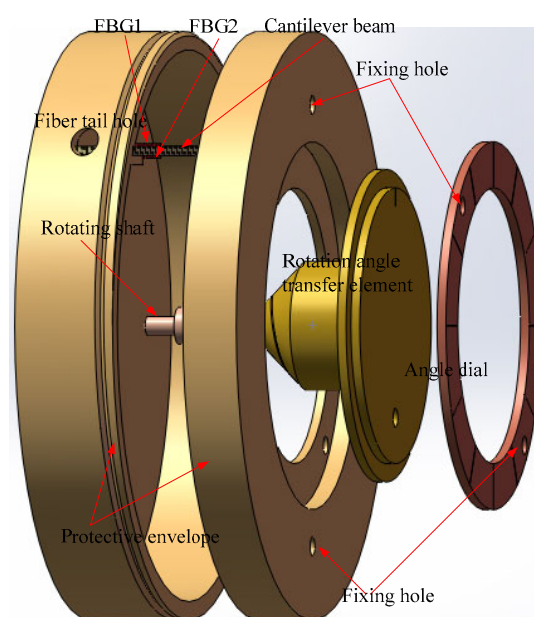


Fig. 1 Composition and structure of the proposed FBG rotation angle sensor.

whose angle interval is 30 degrees is designed to simplify the calibration experiment of this rotation angle sensor. The material of the protective envelop is 304 stainless steel which ensures that this FBG rotation angle sensor can be used in engineering detection.

## 2.2 Theoretical calculation model

Joint working processes of the rotation transfer element, rotating shaft, and triangular cantilever beam are shown in Fig.2. Helical bevel gear on the rotation angle transfer element is designed to restrain the connection line which is marked as  $a$  in

Fig. 2, and its thread turn is 1. As the external rotation angle is  $0^\circ$ , the deflection of the cantilever beam is zero which means that the central wavelengths of FBG1 and FBG2 are not changed. With an increase in the external rotation angle, the deflection increases which leads to the wavelength shifts of FBG1 and FBG2. When the external rotation angle is  $360^\circ$ , the deflection of the cantilever beam goes back to its initial status. So, the proposed FBG sensor can achieve rotation angle measurement with the detection range of  $0 - 2N\pi$  ( $N$  is the positive integer).

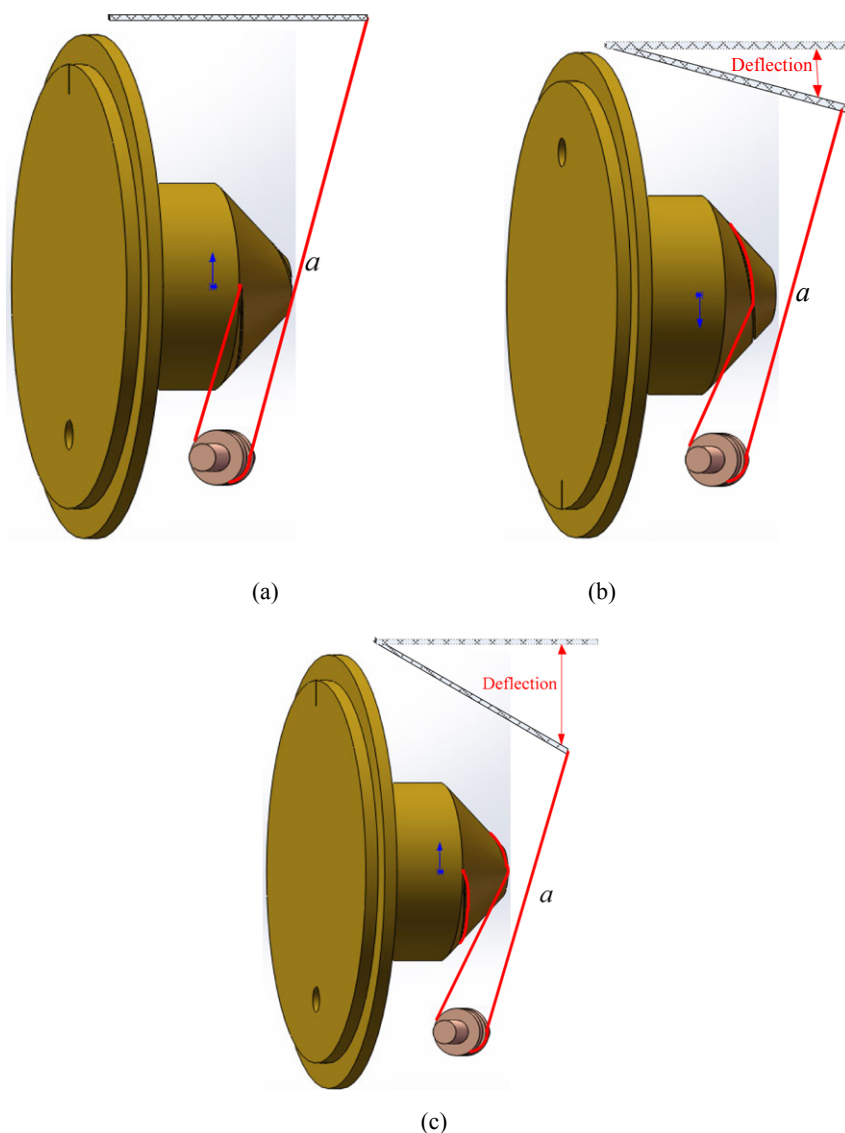


Fig. 2 Joint working processes of the proposed FBG rotation angle sensor: (a) rotation angle  $0^\circ$ , (b) rotation angle  $180^\circ$ , and (c) rotation angle  $360^\circ$ .

Due to the function of the rotation transfer element, the external rotation angle is transferred to its surface displacement change as shown in Fig. 3. The relationship between its surface displacement change  $L_\theta$  and external rotation angle  $\theta$  can be expressed as [9]

$$L_\theta = \int_0^\theta \sqrt{\left[R - (R-r) \cdot \frac{x}{2\pi}\right]^2 + \left(H \cdot \frac{x}{2\pi}\right)^2} dx \quad (1)$$

where  $R$  and  $r$  are the lower and upper surface radii of the cone frustum in the strain transfer element, and  $H$  is its height.

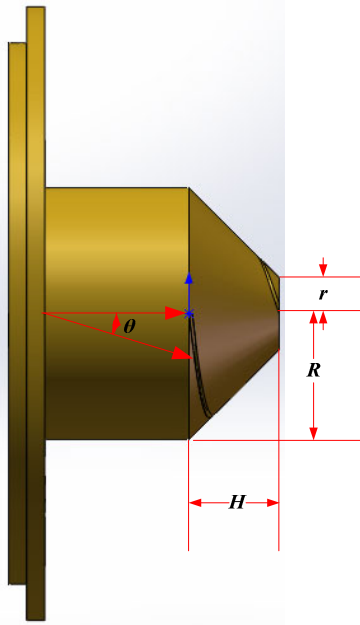


Fig. 3 Rotation transfer element.

Assuming that the connection line is inextensible, the deflection  $y$  of the cantilever beam is [10]

$$y = L_\theta = \int_0^\theta \sqrt{\left[R - (R-r) \cdot \frac{x}{2\pi}\right]^2 + \left(H \cdot \frac{x}{2\pi}\right)^2} dx \quad (2)$$

where the rotation angle range of  $\theta$  is  $2(N-1)\pi - 2N\pi$  ( $N$  is the positive integer).

As the deflection changes, the upper surface tension strain  $\varepsilon_u$  and lower surface compression strain  $\varepsilon_l$  of the cantilever beam which lead to the wavelength shifts of FBG1 and FBG2 are changed. The core sensitive element FBG has wavelength selection characteristics, and only those wavelengths that satisfy the Bragg condition are affected and

strongly back-reflected. The reflected central wavelength  $\lambda_B$  of the FBG can be expressed as [11–13]

$$\lambda_B = 2n_{\text{eff}}\Lambda \quad (3)$$

where  $n_{\text{eff}}$  is the effective index of refraction, and  $\Lambda$  is the grating periodicity of the FBG.

Due to the influence of external temperature and strain on parameters  $n_{\text{eff}}$  and  $\Lambda$ , the reflected wavelength of the FBG is changed as the function of temperature and strain, and their general relationship can be expressed as [14]

$$\begin{cases} \Delta\lambda_{B1} = \lambda_{B1} \cdot (1 - p_\varepsilon)\varepsilon_u + K_T\Delta T \\ \Delta\lambda_{B2} = \lambda_{B2} \cdot (1 - p_\varepsilon)\varepsilon_l + K_T\Delta T \end{cases} \quad (4)$$

where  $\lambda_{Bi}$  ( $i = 1, 2$ ) and  $P_\varepsilon$  are the initial central wavelengths of FBG1 and FBG2 and optical elasticity coefficient, respectively.  $K_T$  is the temperature sensitivity efficient of the FBG, and  $\Delta T$  represents the external temperature changes.  $\varepsilon_u$  is the upper surface tension strain of the cantilever beam, and  $\varepsilon_l$  is the lower surface compression strain. Further, after eliminating the influence of the external temperature through  $\Delta\lambda_{Bi}$  ( $i = 1, 2$ ), the surface strain  $\varepsilon$  of the cantilever beam can be expressed as

$$\varepsilon = (\varepsilon_u - \varepsilon_l)/2 = 1/K_\varepsilon \cdot (\Delta\lambda_{B1} - \Delta\lambda_{B2})/2 \quad (5)$$

where  $K_\varepsilon$  stands for the strain sensitive coefficient of the FBG.

According to the basic knowledge of material and elastic mechanics, the corresponding curve between the deflection  $L_\theta$  and surface strain  $\varepsilon$  of the cantilever beam is

$$L_\theta = l^2/h \cdot \varepsilon = l^2/h \cdot (\varepsilon_u - \varepsilon_l)/2 \quad (6)$$

where  $l$  and  $h$  are the length and height of the cantilever beam. Through combining (2), (5), and (6), the relationship between the wavelength shifts of FBG1 and FBG2  $\Delta\lambda_B$  and external rotation angle can be expressed as follows:

$$\begin{aligned} \Delta\lambda_B &= (\Delta\lambda_{B1} - \Delta\lambda_{B2}) = 2\varepsilon K_\varepsilon = 2K_\varepsilon \cdot h/l^2 \cdot L_\theta \\ &= 2K_\varepsilon \cdot h/l^2 \cdot \int_0^\theta \sqrt{\left[R - (R-r) \cdot \frac{x}{2\pi}\right]^2 + \left(H \cdot \frac{x}{2\pi}\right)^2} dx \end{aligned} \quad (7)$$

So, the external rotation angle  $\theta$  can be obtained by wavelength shifts analyses. The relationship between the wavelength shifts  $\Delta\lambda_B$  and angle  $\theta$  is not linear which means that the detection sensitivity of the proposed FBG rotation angle sensor is not a constant value and varies along with the external rotation angle changes. The characteristics of the detection sensitivity make sure that the relationship between the wavelength shifts and rotation angle is unique under different rotation angles. All these can further improve the measurement precision and rotation angle identification of the FBG rotation angle sensor.

### 3. Calibration experiments

To verify the detection characteristics of the FBG rotation angle sensor, the calibration experiments about the rotation angle and temperature compensation on one prototype are all carried out.

#### 3.1 Rotation angle sensor prototype

Figure 4 displays the prototype of the proposed FBG rotation angle sensor. Material of the protective envelop is 304 stainless steel. Machine oil is chosen as filler to pad the inner gap of the prototype. Machine oil can reduce the influence of external vibration and acts as antioxidant. All these design works make sure that the proposed FBG rotation angle sensor can be used in the harsh engineering detection environment. The geometrical and material parameters of the prototype are all exhibited in Table 1.

#### 3.2 Calibration experimental platform

##### 3.1.1 Rotation angle calibration experiment

The rotation angle calibration experimental platform on the prototype of the proposed FBG rotation angle sensor is made up of the prototype, SM125, and a personal computer, just as shown in Fig. 5. SM125 (demodulation ranges: 1510 nm – 1590 nm, demodulation precision: 1 pm) is chosen as

the fiber interrogator. The prototype can change the rotation angle with a range of  $0^\circ - 1080^\circ$ , and its interval is  $30^\circ$ .  $1080^\circ$  is three times of  $2\pi$  rad and can be used to analyze the periodicity sensitivity of the rotation angle sensor. Personal computer can achieve data acquisition and storage.

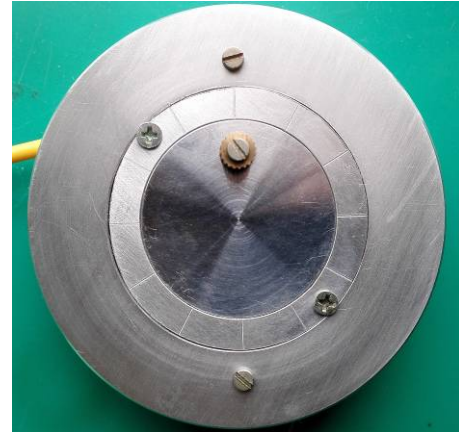


Fig. 4 Prototype of the proposed FBG rotation angle sensor.

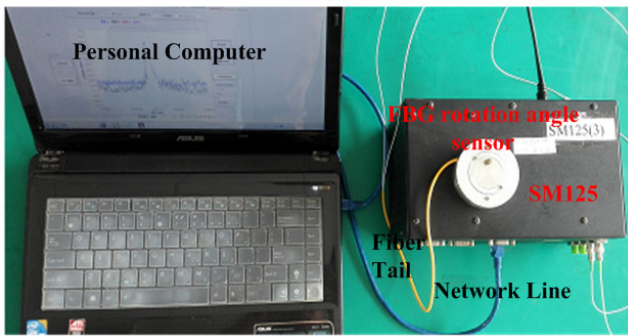
Table 1 Geometrical and material parameters of the prototype.

Symbol	Quantity	Value
$R$	Lower surface radius of cone frustum	5 mm
$r$	Upper surface radius of cone frustum	2 mm
$H$	Height of cone frustum	5 mm
$l$	Length of triangular cantilever beam	30 mm
$h$	Thickness of triangular cantilever beam	0.1 mm
$b_0$	Fixed end length of triangular cantilever beam	10 mm
$\lambda_{B1}$	Initial center wavelength of FBG1	1550.0426 nm
$\lambda_{B2}$	Initial center wavelength of FBG2	1550.1153 nm

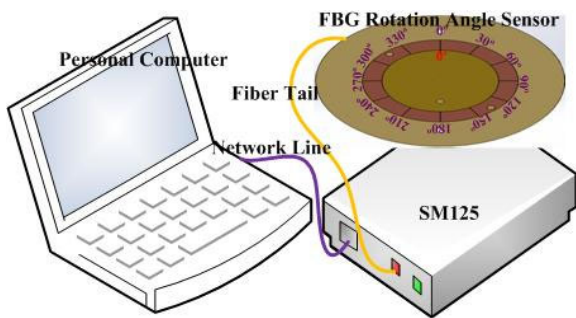
##### 3.1.2 Temperature calibration experiment

In order to obtain the temperature self-compensation performance of this sensor, its temperature calibration experiment is also carried out, and Fig. 6 shows the temperature platform. The temperature range of the constant temperature water tank is from  $-20^\circ\text{C}$  to  $200^\circ\text{C}$ , and its precision is  $0.5^\circ\text{C}$ . The external temperature varies from  $20^\circ\text{C}$  to  $60^\circ\text{C}$  with an interval of  $5^\circ\text{C}$ . The personal computer is used to collect data for ten minutes when the external temperature is stable. The mean

value of the collected data is chosen as the effective data corresponding to each temperature point.



(a)



(b)

Fig. 5 Rotation angle calibration experimental platform: (a) instrument and (b) framework.

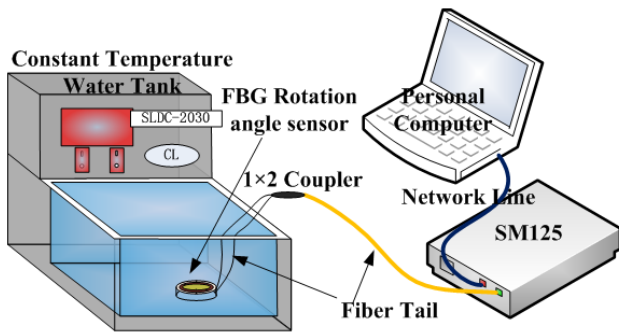


Fig. 6 Temperature calibration experimental platform.

## 4. Data analysis and results

### 4.1 Rotation angle sensitivity analysis

#### 4.1.1 Sensitivity analysis

Table 2 shows the central wavelength experimental data of FBG1 and FBG2 in the rotation angle calibration experiment when the rotation angle changes from 0° to 360° with an interval of 30°.

Table 2 Central wavelength experiment data of FBG1 and FBG2.

Rotation angle (°)	FBG1 (nm)	FBG2 (nm)
0	1550.043	1550.115
30	1550.128	1550.039
60	1550.201	1549.956
90	1550.274	1549.871
120	1550.341	1549.811
150	1550.412	1549.724
180	1550.485	1549.646
210	1550.557	1549.563
240	1550.625	1549.477
270	1550.703	1549.412
300	1550.776	1549.315
330	1550.861	1549.244
360	1550.948	1549.172

Least square method is introduced to analyze the central wavelength experimental data of FBG1 and FBG2. The fitting curves between the central wavelength ( $\lambda_{B1}$  and  $\lambda_{B2}$ ) and external rotation angel ( $\theta$ ) are  $\lambda_{B1} = 0.0025\theta + 1550$  ( $R^2 = 0.9992$ ) and  $\lambda_{B2} = -0.0026\theta + 1550.1$  ( $R^2 = 0.9996$ ).  $R^2$  represents the linearity of the fitting curve. Its value is closer to 1, and the linearity is better. According to the fitting curves, the rotation angle measurement sensitivity coefficients of FBG1 and FBG2 are 2.5 pm/° and 2.6 pm/°, respectively. Further, Fig. 7 shows the relationship between the wavelength shifts  $\Delta\lambda_B$  of the rotation angel sensor and angle  $\theta$ , and their fitting curve is  $\Delta\lambda_B = 0.0049\theta + 0.0056$  ( $R^2 = 0.9994$ ). So, the rotation angle measurement sensitivity coefficient of the rotation angel sensor is 4.9 pm/°. As the wavelength precision of the demodulation instrument SM125 is 1 pm, the measurement precision of the rotation angle sensor is 0.2°. All these experimental data confirm that the proposed rotation angle sensor can achieve the high precision angle measurement with a greater

linearity.

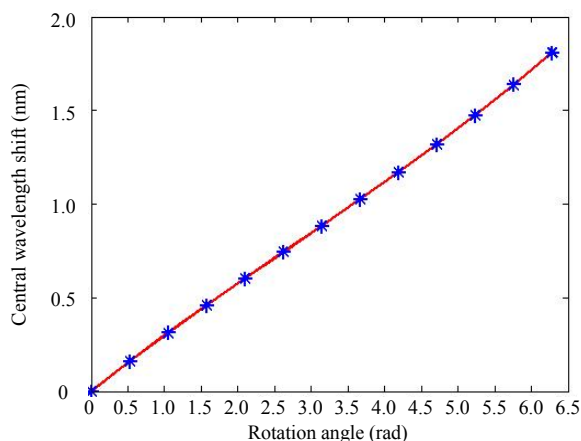


Fig. 7 Corresponding relationship between the wavelength shifts and rotation angle.

#### 4.1.2 Periodicity analysis

Figure 8 shows the central wavelength shifts of FBG1 and FBG2 with the external rotation angle variation in the rotation angle calibration experiment. As the external rotation angle variation is less than  $2\pi$  rad, the central wavelength shifts of FBG1 and FBG2 are monotonically increasing or decreasing. When the rotation angle is bigger than  $2\pi$  rad, the wavelength shifts of FBG1 and FBG2 present the cyclical changes which are displayed in Fig. 8, and the period of the cyclical change is  $2\pi$  rad. These experimental data confirm that the measurement period of the FBG rotation angle sensor is  $2\pi$  rad, and the sensor can almost achieve a boundless range angel measurement.

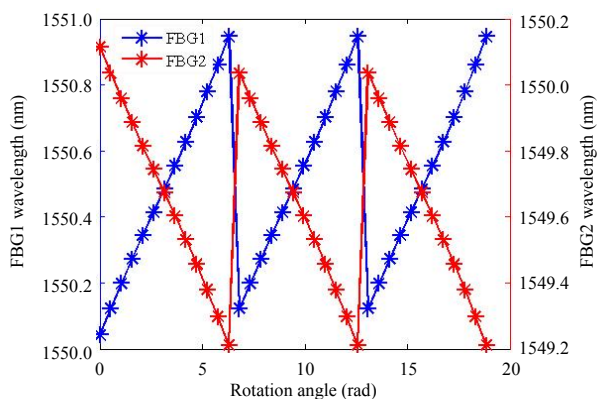


Fig. 8 Central wavelength shifts of FBG1 and FBG2 with the external rotation angle variation.

#### 4.2 Temperature self-compensation performance analysis

Table 3 shows the central wavelength experimental data of FBG1 and FBG2 in the temperature calibration experiment when the temperature of the constant temperature water tank changes from  $20\text{ }^{\circ}\text{C}$  to  $60\text{ }^{\circ}\text{C}$ .

Table 3 Temperature calibration experimental data of FBG1 and FBG2.

External temperature ( $^{\circ}\text{C}$ )	FBG1 (nm)	FBG2 (nm)
20	1550.041	1550.112
25	1550.086	1550.159
30	1550.142	1550.217
35	1550.189	1550.259
40	1550.237	1550.307
45	1550.283	1550.365
50	1550.347	1550.417
55	1550.385	1550.463
60	1550.441	1550.517

The fitting curves between the central wavelength ( $\lambda_{B1}$  and  $\lambda_{B2}$ ) and external temperature ( $T$ ) are  $\lambda_{B1} = 0.01T + 1549.8$  ( $R^2 = 0.999$ ) and  $\lambda_{B2} = -0.0101T + 1549.9$  ( $R^2 = 0.9993$ ), respectively. So, the temperature measurement sensitivity of FBG1 and FBG2 are  $10\text{ pm}/^{\circ}\text{C}$  and  $10.1\text{ pm}/^{\circ}\text{C}$ . Extremely, the similar coefficients of temperature measurement confirm that the FBG rotation angle sensor can achieve the excellent temperature self-compensation.

#### 5. Conclusions

One novel type of miniaturization FBG rotation angle sensor with the high measurement precision and temperature self-compensation which is designed to achieve the rotation angle measurement is proposed and studied in this paper. The FBG rotation angle sensor mainly contains two core sensitivity elements (FBG1 and FBG2), one

triangular cantilever beam, and one rotation angle transfer element. The proposed sensor can achieve self-temperature compensation by two core sensitivity elements (FBG1 and FBG2), and it has a boundless angle measurement range with  $2\pi$  rad period due to the function of the rotation angle transfer element. Based on introducing the joint working processes, the theoretical calculation model of the FBG rotation angle sensor is established, and the rotation angle and temperature calibration experiments on one prototype are all carried out to obtain its measurement performance. The rotation angle calibration experimental results show that the measurement precision of the proposed sensor is  $0.2^\circ$  with the excellent linearity, and the rotation angle measurement sensitivity coefficients of FBG1 and FBG2 are  $2.5 \text{ pm}/^\circ$  and  $2.6 \text{ pm}/^\circ$ , respectively. The periodicity analyses show that the measurement period of the FBG rotation angle sensor is  $2\pi$  rad, and the sensor can almost achieve the boundless range angle measurement. After data analyses, the temperature sensitivities of FBG1 and FBG2 are  $10 \text{ pm}/^\circ\text{C}$  and  $10.1 \text{ pm}/^\circ\text{C}$ , correspondingly. All these experimental data confirm that the FBG rotation angle sensor can achieve the large range angle measurement with the high precision and temperature self-compensation, and it has a certain application value in the rotation angle measurement.

## Acknowledgement

This work is supported by the National 863 Science Foundation of China under Grant No. 2014AA110401.

**Open Access** This article is distributed under the terms of the Creative Commons Attribution 4.0 International License (<http://creativecommons.org/licenses/by/4.0/>), which permits unrestricted use, distribution, and reproduction in any medium, provided you give appropriate credit to the original author(s) and the source, provide a link to the Creative Commons license, and indicate if changes were made.

## References

- [1] T. Chen, W. Q. Zhou, Z. H. Mao, X. Lu, X. Ye, T. C. Huang, *et al.*, "Analysis of the gyro misalignment angle in goniometer based on fiber optic gyroscope," *Optik*, 2016, 127(2): 769–772.
- [2] X. Y. Zhang, M. H. Zhang, and Y. F. Qiao, "A high precision noncontact position measuring system," *Optics & Precision Engineering*, 2002, 10(1): 41–44.
- [3] H. M. Wen and X. H. Ma, "Continuous rotation angles measurement using video frame images," in *Proceeding of 2010 International Conference on ICMT*, Ningbo, China, 2010, pp. 1–5.
- [4] Y. L. Avanesov, K. S. Gorokhovskiy, V. A. Granovskii, M. D. Kudryavtsev, N. K. Kulachenkov, A. E. Angervaks, *et al.*, "Rotation angle measurement device: principle of operation and initial calibration results," in *Proceeding of 2014 11th International Multi-Conference on SSD*, Barcelona, Spain, 2014, pp. 1–6.
- [5] J. A. Kima, J. W. Kim, C. S. Kang, J. H. Jin, and T. B. Eom, "Absolute angle measurement using a phase-encoded binary graduated disk," *Measurement*, 2016, 80: 288–293.
- [6] S. Tao, X. P. Dong, and B. Lai, "Temperature-insensitive fiber Bragg grating displacement sensor based on a thin-wall ring," *Optics Communications*, 2016, 372: 44–48.
- [7] G. Pereira, M. McGugan, and L. P. Mikkelsen, "Method for independent strain and temperature measurement in polymeric tensile test specimen using embedded FBG sensors," *Polymer Testing*, 2016, 50: 125–134.
- [8] S. Hannusch, M. Stockmann, and J. Ihlemann, "Experimental method for residual stress analysis with fibre Bragg grating sensors," *Materials Today: Proceedings*, 2016, 3(4): 979–982.
- [9] R. Paine, C. Beards, P. Tucker, and D. H. Bacon, *Mechanical engineer's reference book*. Amsterdam, Holland: Elsevier, 1994: 1–48.
- [10] L. J. Vandepierre, X. Wang, and A. Atkinson, "Measurement of mechanical properties using slender cantilever beams," *Journal of the European Ceramic Society*, 2016, 36(8): 2003–2007.
- [11] A. I. H. Serrano, G. S. Delgado, D. M. Hernandez, A. M. Rios, and D. M. Hernandez, "Robust optical fiber bending sensor to measure frequency of vibration," *Optics and Lasers in Engineering*, 2013, 51(9): 1102–1105.
- [12] X. L. Zhang, P. Wang, D. K. Liang, C. F. Fan, and C. L. Li, "A soft self-repairing for FBG sensor network



- in SHM system based on PSO-SVR model reconstruction,” *Optics Communications*, 2015, 343: 38–46.
- [13] Y. Cao, H. Y. Liu, Z. R. Tong, S. Yuan, and J. Su, “Simultaneous measurement of temperature and refractive index based on a Mach-Zehnder interferometer cascaded with a fiber Bragg grating,” *Optics Communications*, 2015, 342: 180–183.
- [14] C. Li, T. G. Ning, X. D. Wen, J. Li, J. J. Zheng, H. D. You, *et al.*, “Strain and temperature discrimination using a fiber Bragg grating and multimode interference effects,” *Optics Communications*, 2015, 343: 6–9.